# Quantification of transcription factor binding in cell extracts using an electrochemical, structure-switching biosensor

Andrew J. Bonham, Kuangwen Hsieh, B. Scott Ferguson,
Alexis Vallée-Bélisle, Francesco Ricci, H. Tom Soh, Kevin W. Plaxco

**Electrochemical methods:**
Square-wave voltammetric determinations were performed using a CH Instruments 650C potentiostat, scanning from 0 V to -0.5 V with an increment of 1 mV, an amplitude of 50 mV, and a frequency of 60 Hz. Initial experiments were performed at frequencies ranging from 10 Hz to 2000 Hz, and optimal signal change upon protein binding was seen at 60 Hz.

**Non-optimal sensor designs:**
Several additional conformation-switching variant structures were investigated for their ability to form an electrochemically response structure-switching sensor, including those with similar conformations as the solution-based TF beacons and those with a simplified, helix "sliding" mechanism. We include these structures to highlight that a key enabling feature of the final sensor design is the double-helical region separating the methylene blue from the surface in the signal-off state; designs which relied upon a single-stranded region to fulfill this purpose displayed poor signal gain, which we attribute to the extreme flexibility of single-stranded DNA tethered to a gold surface, allowing the methylene blue to freely transfer electrons.

*Figure S1: Background current levels of explored sensor geometries.* High background current of alternate geometries 1 and 2 contributed to the lack of discernible change in current in the presence of target.
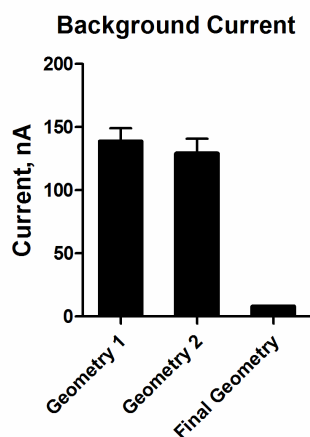


*Figure S2: Alternate oligonucleotide geometry 1:*
This sensor geometry is fundamentally the same as the folding pattern used for the solution based TF beacons (Vallée-Bélisle, A.; Bonham, A. J.; Reich, N. O.; Ricci, F.; Plaxco, K. W. Transcription Factor Beacons for the Quantitative Detection of DNA Binding Activity. *J Am Chem Soc* 2011, *133*, 13836.). It displayed inconsistent behavior, which we hypothesize may stem from the relatively small change in the distance from the surface that the methylene blue experiences in the different conformations. Here, the structure on the left is the binding competent state, and the structure on the right is the non-binding state.

5'- Thiol- TAC CTT TAT ATA AAT AGG TT(mb)G TGA TTT TTA TAT ATT TCA C -3'
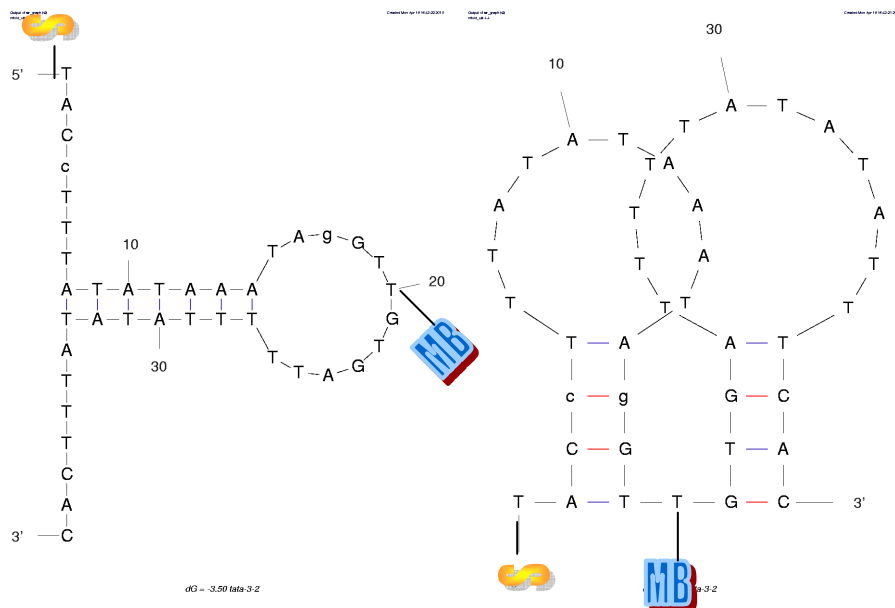


*Figure S3: Alternate oligonucleotide geometry 2:*
This sensor geometry was based on the principle of alternate folds that could "slide" along the sequence. Although it gave a signal-on response, it was not a large or robust signal change. We hypothesize that this is due to the inherent flexibility of the single-stranded region that separates that methylene blue from the surface in the "off" state. Here, the structure on the right is the binding competent state, and the structure on the left is the non-binding state.
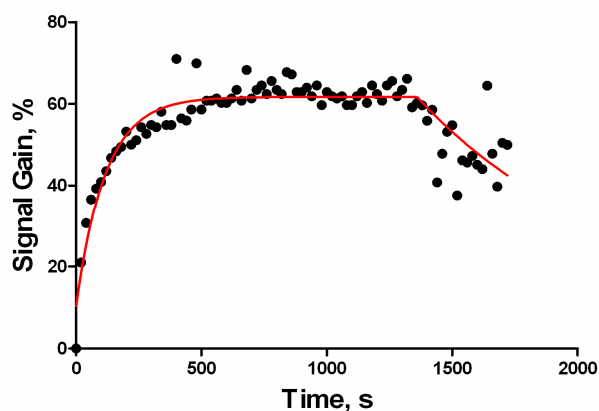
Sequence:
5'- Thiol- TTTGAATATATTTTACCCGACGAAAATATATTCGT(mb)CGG -3'
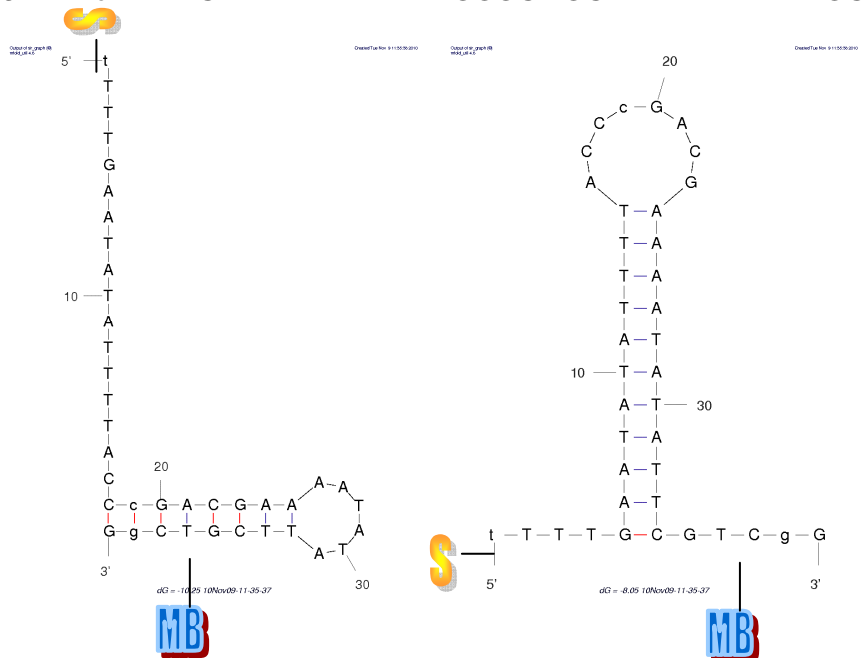
Structures generated by mfold web server, http://mfold.rna.albany.edu. M. Zuker, Mfold web server for nucleic acid folding and hybridization prediction. Nucleic Acids Res. 31 (13), 3406-3415, 2003)

*Figure S4:  Kinetic measurements of association and dissociation.*



The kinetic response of our electrochemical sensor was assessed by performing repeated scans at 10 second intervals after addition of a saturating amount of TBP (500 nM) was introduced to the buffer (sensor was pre-equilibrated in buffer).  After response current had stabilized, the solution was changed to pure buffer to induce dissociation of bound TF.  Fitting this data to an "association, then dissociation" model with GraphPad Prism software (Graphpad, San Diego, CA) revealed a $k_{on}$ and $k_{off}$ consistent with prior measurements of TBP binding, and these constants were used to calculate an apparent thermodynamic dissociation constant, $K_D$, of $110 \pm 24$ nM, in strong agreement with our thermodynamic data ($121 \pm 20$ nM).

**Microfluidic chip fabrication and cleaning:**

For the electrode substrate, platinum reference and counter electrodes and gold working electrodes were sequentially microfabricated on a 4-inch-diameter, 500-µm-thick borofloat glass wafer (Mark Optics, Santa Ana, CA) through successive standard lift-off processes. The lift-off consisted of transparency mask (Grayphics, Santa Barbara, CA) based contact photolithography, electron-beam evaporation based metal deposition (180 nm of platinum or gold on 20 nm titanium for adhesion; VES 2550, Temescal, Livermore, CA), and immersion and gentle sonication in acetone. The chamber layer was comprised of a 250-µm-thick PDMS sheet (BISCO Silicones, Rogers Corporation, Carol Stream, IL) with the channel design cut by a programmable sign-cutting tool (CE5000-60, Graphtec, Santa Ana, CA). For the fluidic via substrate, eyelet holes were drilled through a second borofloat glass wafer by an 1.1-mm-diameter diamond drill bit (Triple Ripple, Abrasive Technology, Lewis Center, OH) using a programmable CNC milling machine (Flashcut CNC, San Carlos, CA). The electrode wafer and the fluidic via wafer were diced (Disco DAD-2H/6, Tokyo, Japan) into individual chips prior to assembly.

The three modular layers were manually assembled in a fume hood. During the assembly, one side of the PDMS layer was corona treated with a high-frequency emitter (BD-20AC, Electro-Technic Products, Chicago, IL) for approximately 5 seconds before being bonded to the fluidic via substrate. This assembly was allowed to rest for several minutes to ensure strong bonding between PDMS and glass. Subsequently, the other side of the PDMS was corona treated and bonded to the electrode substrate. The gold working electrode in each assembled chip was cleaned in 50 mM $H_2SO_4$ via cyclic voltammetry, with twelve potential sweeps ranging from -0.8 to 1.0 V (with respect to the platinum reference electrode) applied at 0.1 V s$^{-1}$ with a sample interval of 0.001 V and 10 µA sensitivity, readying it for DNA probe immobilization.